*munol.* **144**, 1696 (1990).
5. P. S. Linsley and J. A. Ledbetter, *Annu. Rev. Immunol.* **11**, 191 (1993); C. H. June, J. A. Bluestone, L. M. Nadler, C. B. Thompson, *Immunol. Today* **15**, 321 (1994).
6. H. Groux *et al.*, *J. Exp. Med.* **175**, 331 (1992); L. H. Boise *et al.*, *Immunity* **3**, 87 (1995).
7. B. L. Levine, Y. Ueda, N. Craighead, M. L. Huang, C. H. June, *Int. Immunol.* **7**, 891 (1995); B. L. Levine, N. Craighead, T. Lindsten, C. B. Thompson, C. H. June, unpublished data.
8. B. L. Levine *et al.*, data not shown.
9. B. L. Levine, J. D. Mosca, J. L. Riley, R. G. Carroll, O. S. Weislow, D. C. St. Louis, C. H. June, unpublished data.
10. Culture with CD3 and CD28 mAbs provides a proliferative advantage for $CD4^+$ over $CD8^+$ lymphocytes with uninfected donors (*7*) [R. Costello *et al.*, *Eur. J. Immunol.* **23**, 608 (1993)]. However, with HIV-infected donors, the proportion of $CD28^-$ lymphocytes is greater and there are more $CD8^+$ lymphocytes in the input culture, so that further enrichment steps would be required to obtain pure $CD4^+$ lymphocytes at culture termination.
11. $T_H1$ cytokines predominate in cell cultures when immobilized CD28 mAb is used for stimulation (*7*). In contrast, when soluble CD28 mAb is used for cell culture, $T_H2$ cytokines may predominate [C. L. King, R. J. Stupi, N. Craighead, C. H. June, G. Thyphronitis, *Eur. J. Immunol.* **25**, 587 (1995); W. Holter, O. Majdic, F. S. Kalthoff, W. Knapp, *ibid.* **22**, 2765 (1992); T. van der Pouw Kraan, R. de Jong, L. Aarden, *ibid.* **23**, 1 (1993)]. In vivo, CD28-B7 blockade after alloantigenic challenge inhibits $T_H1$ cytokines but spares $T_H2$ cytokines [M. H. Sayegh *et al.*, *J. Exp. Med.* **181**, 1869 (1995)]. Thus, the mode of CD28 stimulation may affect $T_H1$ and $T_H2$ development [J. A. Bluestone, *Immunity* **2**, 555 (1995); C. B. Thompson, *Cell* **81**, 979 (1995)].
12. Cytokine secretion was tested in cultures from eight patients in Table 1 after 10 to 20 days in culture. Cells were collected and washed, and the extent of cytokine secretion upon restimulation was determined by placing the cells into fresh medium with beads coated with CD3 and CD28 mAbs for 24 hours. Cell-free culture supernatants were analyzed for IL-2, IFN-γ, IL-4, IL-5, and TNF-α by ELISA with the use of commercially available kits [T Cell Diagnostics, Woburn, MA (IL-2); R&D Systems, Minneapolis (TNF-α, IL-4, and IL-5); Endogen, Boston (IFN-γ)].
13. F. Cocchi *et al.*, *Science* **270**, 1811 (1995).
14. B. Asjo, D. Cefai, P. Debre, Y. Dudoit, B. Autran, *J. Virol.* **67**, 4395 (1993); M. D. Smithgall, J. G. P. Wong, P. S. Linsley, O. K. Haffar, *AIDS Res. Hum. Retroviruses* **11**, 885 (1995); L. M. Pinchuk, P. S. Polacino, M. B. Agy, S. J. Klaus, E. A. Clark, *Immunity* **1**, 317 (1994).
15. CD4 cells have a hierarchy of permissiveness to HIV-1 infection that is determined by the mode of stimulation with various mitogens. In most donors, the susceptibility to HIV-1 infection is [soluble CD3 mAb, soluble CD28 mAb] → [concanavalin A, PHA] → [immobilized CD3 mAb, soluble CD28 mAb] → [immobilized CD3 mAb, immobilized CD28 mAb]. The increased susceptibility of CD4 cells to HIV infection after stimulation with soluble antibody has been noted previously (*14*).
16. J. A. Nunes, Y. Collette, A. Truneh, D. Olive, D. A. Cantrell, *J. Exp. Med.* **180**, 1067 (1994); J. A. Ledbetter *et al.*, *Blood* **75**, 1531 (1990).
17. We have considered whether the antiviral effect mediated by CD28 costimulation might be a soluble factor or factors previously described by others [C. M. Walker, D. J. Moody, D. P. Stites, J. A. Levy, *Science* **234**, 1563 (1986)]. Given that the factor first described by Levy is secreted by CD8 cells and suppresses viral replication late in the viral life cycle, it is likely that the CD28 effect we have described is distinct. First, as shown in Table 2, the effect mediated by CD28 requires <0.6% CD8 cells, and thus it is either independent of CD8 T cells or dependent on trace amounts of CD8 cells. Second, the CD28 effect acts early in the viral life cycle to prevent infection of CD4, whereas the effect first described by Levy is reported to act late in the viral life cycle to suppress infection. Third, Cocchi *et al.* (*13*) have reported that chemokines are the major mediator of the CD8 antiviral effect, and we have found that the secretion of C-C chemokines is not dependent on CD28 stimulation (*9*).
18. A. Cayota, F. Vuillier, D. Scott-Algara, V. Feuillie, G. Dighiero, *Clin. Exp. Immunol.* **91**, 241 (1993).
19. N. Weng, B. L. Levine, C. H. June, R. J. Hodes, *Proc. Natl. Acad. Sci. U.S.A.* **92**, 11091 (1995); C. H. June, J. A. Ledbetter, M. M. Gillespie, T. Lindsten, C. B. Thompson, *Mol. Cell Biol.* **7**, 4472 (1987).
20. D. Dobrescu *et al.*, *Proc. Natl. Acad. Sci. U.S.A.* **92**, 5563 (1995); J. Laurence, A. S. Hodtsev, D. N. Posnett, *Nature* **358**, 255 (1992).
21. TCR $V_\beta12$ analysis was done by flow cytometry on four paired cultures of CD4 cells from patients shown in Table 1 before and after 3 to 5 weeks in culture. The $V_\beta12$ population was 1.0 ± 0.4% on day 0 and 2.8 ± 1.4% at the end of the culture period (mean ± SD, $P = 0.18$).
22. N. J. Borthwick *et al.*, *AIDS* **8**, 431 (1994); J. E. Brinchmann *et al.*, *J. Infect. Dis.* **169**, 730 (1994); D. E. Lewis, D. S. Tang, A. Adu-Oppong, W. Schober, J. R. Rodgers, *J. Immunol.* **153**, 412 (1994).
23. E. Maggi *et al.*, *Science* **265**, 244 (1994).
24. C. C. Wilson *et al.*, *J. Infect. Dis.* **172**, 88 (1995).
25. The CD4 percentage on day 0 of culture was not obtained for patients 5 and 9 because of limited cell availability; thus, the calculated cell proliferation is the actual cell proliferation without correction for the CD4 count, because only the final CD4 percentage was available.
26. M. T. Vahey, M. T. Wong, N. L. Michael, in *PCR Primer: A Laboratory Manual*, C. W. Dieffenbach and G. S. Dveksler, Eds. (Cold Spring Harbor Laboratory Press, Cold Spring Harbor, NY, 1995), p. 17; M. T. Vahey and M. T. Wong, in *ibid.*, p. 313; N. L. Michael, M. Vahey, D. S. Burke, R. R. Redfield, *J. Virol.* **66**, 310 (1992).
27. S. Gartner *et al.*, *Science* **233**, 215 (1986); J. R. Mascola *et al.*, *J. Infect. Dis.* **169**, 48 (1994).
28. Supported by Army and Naval Medical Research and Development Commands grant 1437 and NIH grant AI29331. We thank W. Bernstein and J. Lin for intellectual and experimental contributions; C. Thompson for manuscript review; D. Ritchey, S. Perfetto, D. Smoot, N. Craighead, J. Cotte, and S. Barrick for technical assistance; J. D. Malone and J. L. Malone for support and encouragement; clinic patients for blood donation; P. Ganong (Boehringer Ingelheim, Ridgefield, CT) for Nevirapine; and N. Peterson (Ortho Biotech, Raritan, NJ) for CD3 mAb OKT3. The views expressed in this report are those of the authors and do not reflect the official policy or position of the Departments of the Navy and Army, the Department of Defense, or the U.S. government.

19 December 1995; accepted 10 May 1996

# Solution Structure of a Two-Base DNA Bulge Complexed with an Enediyne Cleaving Analog

Adonis Stassinopoulos,* Jie Ji, Xiaolian Gao,† Irving H. Goldberg†

Nucleic acid bulges have been implicated in a number of biological processes and are specific cleavage targets for the enediyne antitumor antibiotic neocarzinostatin chromophore in a base-catalyzed, radical-mediated reaction. The solution structure of the complex between an analog of the bulge-specific cleaving species and an oligodeoxynucleotide containing a two-base bulge was elucidated by nuclear magnetic resonance. An unusual binding mode involves major groove recognition by the drug carbohydrate unit and tight fitting of the wedge-shaped drug in the triangular prism pocket formed by the two looped-out bulge bases and the neighboring base pairs. The two drug rings mimic helical DNA bases, complementing the bent DNA structure. The putative abstracting drug radical is 2.2 ± 0.1 angstroms from the pro-*S* H5′ of the target bulge nucleotide. This structure clarifies the mechanism of bulge recognition and cleavage by a drug and provides insight into the design of bulge-specific nucleic acid binding molecules.

Bulged structures (regions of unpaired bases) in nucleic acids have been the subject of intense interest (*1*), because they have been implicated as binding motifs for regulatory proteins in viral replication (*2*), as targets for repair enzymes in imperfect homologous recombination (*3*), as products of slipped mispairing in the replication of microsatellite DNA (*4*), as intermediates in frameshift mutations (*5*), and as essential elements in naturally occurring antisense RNAs (*6*).

Neocarzinostatin chromophore (NCS chrom) is unusual among the naturally occurring enediyne antibiotics (*7*) in its ability to attack specifically and exclusively a single residue at a two-base bulge of certain DNA sequences under the influence of general base catalysis (*8*). Under the same conditions NCS chrom cleaves the transactivation response element of human immunodeficiency virus type I viral RNA with high specificity at one of its proposed bulge residues (*9*). Further, studies with long single-stranded DNAs, similar to ones found in some DNA viruses, have revealed related binding-cleavage sites located at bulged sites (*10*). This

A. Stassinopoulos and I. H. Goldberg, Department of Biological Chemistry and Molecular Pharmacology, Harvard Medical School, Boston, MA 02115, USA.
J. Ji and X. Gao, Department of Chemistry, University of Houston, Houston, TX 77204–5641, USA.

*Present address: Steritech Incorporated, Suite 300, 2525 Stanwell Drive, Concord, CA 94520, USA.
†To whom correspondence should be addressed.

mode of binding and attack is, therefore, an attractive candidate in the design of antiviral drugs specific for bulged features in DNA and RNA.

The reaction with DNA bulges is initiated by an intramolecular nucleophilic attack of C1″ at C12 of NCS chrom **1**, resulting in the sequential formation of the labile spirolactone-containing intermediates cumulene **2** and biradical **3** (Fig. 1A). The biradical **3** is ultimately responsible for DNA damage by hydrogen atom abstraction at the bulged site and production of **4** (*11*). Compound **5** (designated NCSi-gb), produced by the general-base–catalyzed activation of NCS chrom in the absence of DNA, is a stable structural analog of the labile cleaving species and binds specifically at this bulged site (*12*). A model of NCSi-gb demonstrates that the two ring systems NA and THI are held rigidly at an angle of 60° (as measured by their short axes) by the five-member spirolactone to form a wedge with two flexible appendices, *N*-methyl fucosamine (NMF) and cyclocarbonate moieties.

To understand the molecular basis for the recognition of the bulged structure, we determined the solution structure of the complex formed between the stable compound NCSi-gb and an oligonucleotide containing the known binding-cleavage site 5′ AA*T*T·AT 3′ (bulged residues in italics, attacked residue in bold) (Fig. 1B) (*13*). The construct was designed on the basis of previous work (*8*–*12*) and consists of 8- and 10-nucleotide oligomers connected by means of a chemical linker (*14*). The two-base bulge, flanked by a minimum of three base pairs on each side, is a substrate for the cumulene **2** and binds NCSi-gb (with a dissociation constant, $K_d$, of 3.9 μM) (*12*).

Initial titration experiments, as monitored by one-dimensional (1D) nuclear magnetic resonance (NMR) spectra, confirmed the formation of a stable 1:1 complex on mixing of the DNA construct with NCSi-gb (10 mM sodium phosphate, pH ≈ 6). The resonances for most $^1$H in both free DNA and the complex and those of $^{31}$P of the complex were assigned with established procedures (*15*) on the basis of correlated spectroscopy (COSY) and nuclear Overhauser effect spectroscopy (NOESY) experiments. They are mostly characteristic of a right-handed helical duplex and follow typical through-bond and through-space connectivities (*16*). The assignments of the 1D and 2D NOESY NMR spectra of the complex (10% $D_2O$ in $H_2O$) showed the presence of eight Watson-Crick base-paired imino protons and an additional non–base-paired imino proton, assigned to T13, consistent with the proposed structure (Fig. 1B) (*17*). Further analyses established that all DNA residues adopt the antiglycosidic conformation (*16*). Several NOE irregularities at and around residues A5, A11, and T13 confirmed the disruption of the double-helical structure in the complex (*17*). Of the observed intermolecular contacts, 85% are between NCSi-gb and the A11-A12-T13-T14 strand, confirming the binding at the bulge site A12-T13. A distinct feature of the complex is the lack of

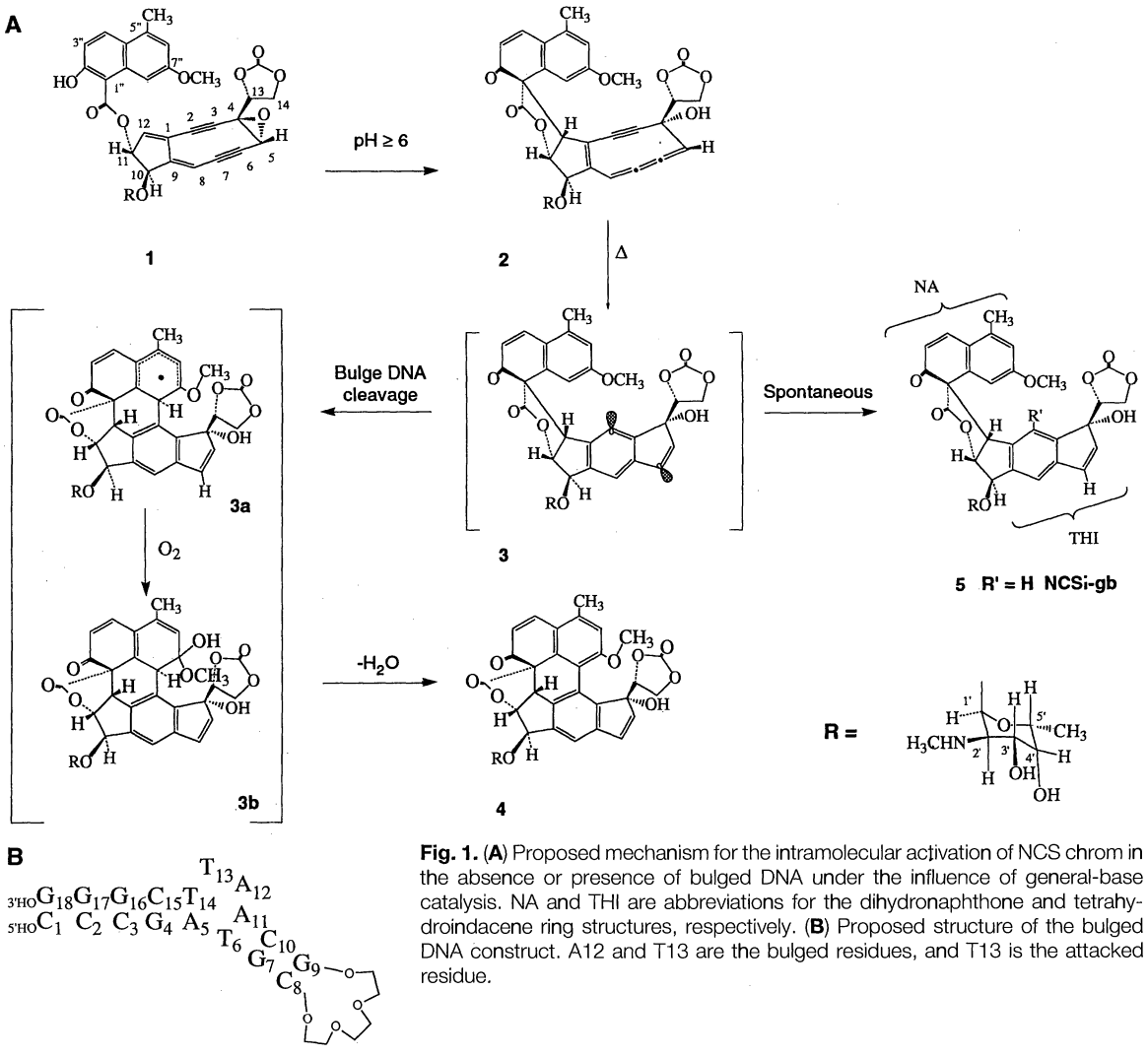


**Fig. 1.** (**A**) Proposed mechanism for the intramolecular activation of NCS chrom in the absence or presence of bulged DNA under the influence of general-base catalysis. NA and THI are abbreviations for the dihydronaphthone and tetrahydroindacene ring structures, respectively. (**B**) Proposed structure of the bulged DNA construct. A12 and T13 are the bulged residues, and T13 is the attacked residue.

interactions between NCSi-gb with duplex H1's, which are located in the minor groove in a right-handed helix and are the major contact sites for most molecules that bind in the minor groove (*18*). The absence of these interactions distinguishes NCSi-gb from the minor groove–binding molecules, implicating an unusual mode of DNA recognition by this molecule.

The high-resolution structure of the NCSi-gb·DNA complex (Fig. 2) was elucidated with distance geometry and molecular computations, on the basis of a total of 629 NMR restraints (including 85 intermolecular NOEs) (*19*–*21*). The structures were optimized iteratively and the final complete relaxation matrix refinement statistics determined (*22*). The final structures show excellent agreement with the experimental data and satisfactory coordinate convergence and chemical bond geometry (Fig. 2A) (*21*).

The energy-minimized structures (Fig. 2) exhibit unprecedented features, notably recognition of the bulge site by NCSi-gb from the major groove. The two rigidly held ring systems of NCSi-gb form a molecular wedge that penetrates the binding pocket and immobilizes the otherwise flexible bulged A12 and T13 residues (Fig. 2, B and C) (*23*). The drug ring systems each stack on the DNA base pairs that define the long sides of the triangular prism binding pocket (Fig. 2B). The two ring systems of NCSi-gb mimic the geometry of helical bases with a twist angle of ~35° (measured by the long axes) and a rise of ~3 Å at the narrower end and mediate the helical transition between the two half helices on either side of the bulge (Fig. 2B) (*24*).

Stacking interactions among the aromatic moieties play an important role in stabilizing the NCSi-gb complex. The NA ring interacts with the A11-T6 base pair through stacking, mainly over A11, so that the NA and A11 long axes are perpendicular to one another. These results were established by the NOEs connecting H6″, H8″, and 7″-methyl (Me) from the second ring of NA with A11 H2, A12 H8, and their sugar protons; 5″-Me with the T6 imino and A11 H2 protons; and H3″ and H4″ from the first ring of NA with A5 H8. The carbonyl of the spirolactone ring at the closed end of the molecular wedge is placed along the major groove, pointing toward the aromatic system of A11. The THI ring system is partially stacked under the T14-A5 base pair, with their long axes being almost perpendicular (Fig. 2, A and B). The THI system, located above the A12 sugar, causes an upfield shift of the A12 proton resonances, and interproton contacts can be seen between THI and the A12-T13 backbone. The 4-OH of THI can hydrogen bond either to the adjacent cyclocarbonate O17 or the 3′-phosphate of A12. H5 and H6 of THI show NOEs to the H5′/H5″ of T13 and T14, and H8 is in close contact with the methyl group of T14, placing this edge of the THI system close to T13 and T14. The cyclocarbonate ring interacts with the T14-A5 base pair and causes a disruption of the in-plane alignment of the T14-A5 base pair. This suggests that removal of the cyclocarbonate group might actually improve the binding at this site.

The major groove recognition is carried out by the NMF moiety, which sits in the center of the major groove, unlike most aminoglycosides of other DNA binding drugs that usually recognize the sugar-phosphate backbone through the minor groove (Fig. 2A) (*18*). NMF acts as an anchor, determining how deep into the major groove NCSi-gb can penetrate. NMF makes contacts with protons of the A5-T14 base pair using the side containing H3′, H4′, and H5′ (and the 5′-Me), and the 2′-NMe group extends close to H8 of G4 in the major groove. This face of NMF is also in the proximity of the A12-

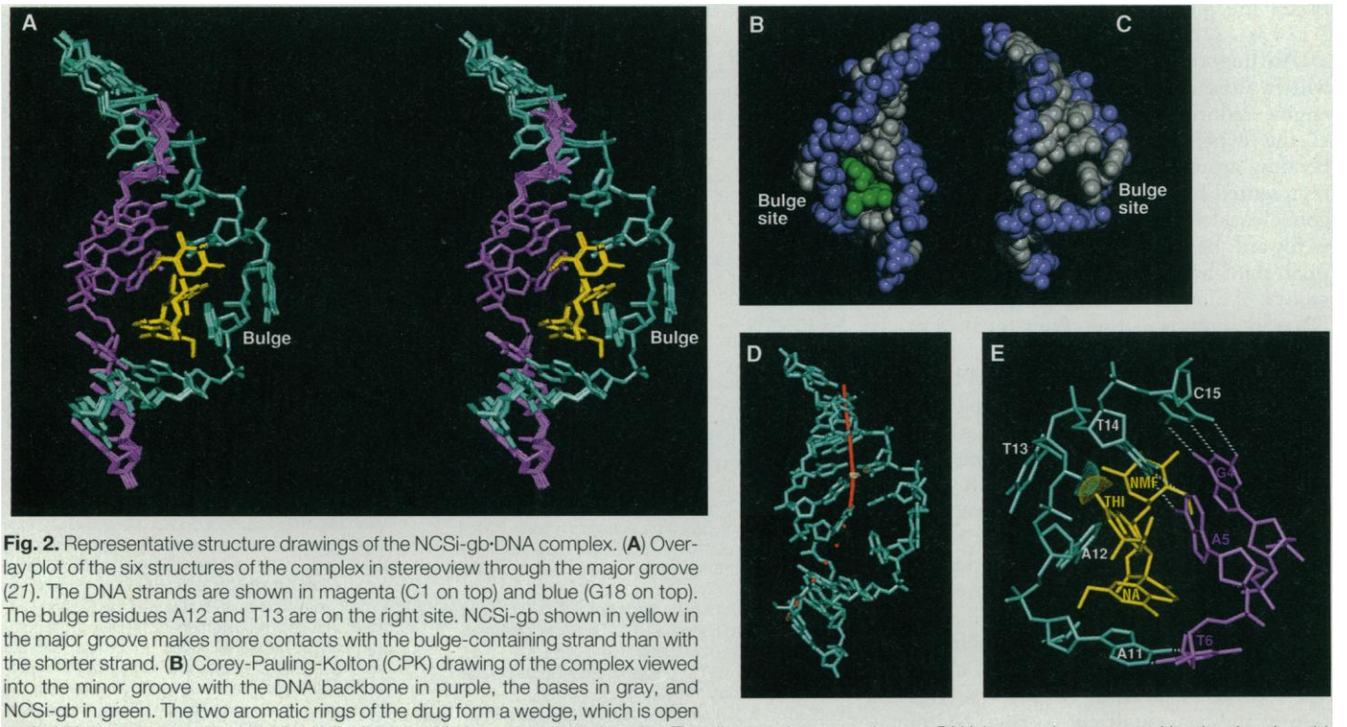


**Fig. 2.** Representative structure drawings of the NCSi-gb·DNA complex. (**A**) Overlay plot of the six structures of the complex in stereoview through the major groove (*21*). The DNA strands are shown in magenta (C1 on top) and blue (G18 on top). The bulge residues A12 and T13 are on the right site. NCSi-gb shown in yellow in the major groove makes more contacts with the bulge-containing strand than with the shorter strand. (**B**) Corey-Pauling-Kolton (CPK) drawing of the complex viewed into the minor groove with the DNA backbone in purple, the bases in gray, and NCSi-gb in green. The two aromatic rings of the drug form a wedge, which is open to the minor groove, and mimic the helical nucleotide bases at the bulge site. The distance between the two DNA base pairs separated by the drug is ~11 Å. The cyclic carbonate has been removed for clarity. (**C**) The triangular prism binding pocket in the DNA duplex shown in a CPK drawing, viewed from the major groove. NCSi-gb is not shown. (**D**) Drawing showing the helical axis (in red) of the duplex (in blue) in the complex. The bending angle between the two half helices as projected in the drawing plane is about 45°. (**E**) Drawing showing the binding and the cleavage site from the minor groove with A11-A12-T13-T14-C15 in blue, G4-A5-T6 in magenta, and NCSi-gb in yellow. The binding pocket consists of the bases from A5·T14, T6·A11, and bulge A12 and T13 residues. The 2.2 ± 0.1 Å separation between C6 radical of NCSi-gb and T13 pro-*S*–H5′ is demonstrated by their van der Waals dot surface drawings.

T13 bulge backbone, as indicated by NOEs to A12 H2 and T13 H1′. These DNA protons point toward the minor groove in a right-handed helix, so that the observed NOEs to the drug NMF protons, located in the major groove, reflect a distorted phosphate backbone for the A12 and T13 residues. The interactions of the drug with A5-T14 and G4 are consistent with the sensitivity of the cleavage reaction, and thus the binding, to the residues flanking the bulge (*8*). The two NMF hydroxyls are exposed to the solvent .

The binding of NCSi-gb locks the conformation of the two bulge residues (A12 and T13) in a looped-out position in the major groove with antiglycosidic conformations and their bases oriented nearly orthogonal to those in the helix (Fig. 2C) (*23*). This arrangement places their hydrophilic edge toward the solvent and their hydrophobic edge toward the binding site. They help enclose the drug inside the binding site, further defining the outer limits of the triangular prism binding site, which is narrower when viewed from the major groove than from the minor groove. The conformation of T13 appears to be stabilized by hydrophobic interactions of the aromatic system with the 5′-Me of NMF, as indicated by the observed NOEs. Hydrophobic interactions are also observed between the methyl group of T13 and the A12 base.

An important feature of the complex, which, although predicted (*1*, *25*), was not engineered in the iterative efforts to model the experimental data, is the ~45° bending around the bulge binding site as represented by the central axis of the oligonucleotide (Fig. 2D). The bent axis faces toward the shorter strand and displays a small right-handed twist toward the major groove. Although the arrangement of free DNA is unknown, the characteristics of the bent NCSi-gb·DNA complex agrees with those described in intrahelical bulge DNA sequences (*25*), demonstrating that NCSi-gb is a model compound that possesses the right geometry for mimicking natural helical bases. This molecule, featuring rigidly held unsaturated ring systems, is a relatively simple synthetic target and should serve as an example for designing molecular probes specific for nucleic acid bulges (*26*).

The structure of the complex has implications for the observed bulge DNA cleavage and the mechanism of bulge recognition in the base-catalyzed reaction. NCSi-gb shares with its precursor cumulene **2** a rigid wedge-shaped body as a result of the presence of the spirolactone ring and is virtually isostructural to biradical **3**, the species ultimately responsible for the reactions leading to both the DNA damage and the formation of **4**. Because **4** does not bind to this sequence (*12*), this structure provides a glimpse of the productive complex before the hydrogen abstraction. Consistent with this is the short distance between the C6 radical and the substrate T13 (pro-*S*) H5′ proton (2.2 ± 0.1 Å), which is abstracted during DNA damage (Fig. 2E) (*8*). The observed arrangement of NCSi-gb within the binding-cleavage site further indicates that the cumulene **2**, rather than the parent NCS chrom compound, is the species responsible for the molecular recognition of the bulge site, consistent with previous data (*11*). Furthermore, the total inclusion of NCSi-gb in the binding pocket makes the solvent quenching of the C2 radical sterically hindered. This may explain the efficient formation of **4** in the presence of bulged DNA, as the exclusion of solvent makes the electrophilic addition of the C2 radical on C8″ to form the C2-C8″ bond the most likely reaction (*27*). Finally, the structure explains why bulges that contain only a single or as many as five residues are not substrates for the cleavage reaction (*8*).

## REFERENCES AND NOTES


1. D. H. Turner, *Curr. Opin. Struct. Biol.* **2**, 334 (1992); M. J. Lilley, *Proc. Natl. Acad. Sci. U.S.A.* **92**, 7140 (1995), and references therein.
2. S. Feng and E. C. Holland, *Nature* **334**, 165 (1988); C. Dingwall *et al.*, *EMBO J.* **9**, 4145 (1990); M. J. Gait and J. Karn, *Trends Biochem. Sci.* **18**, 255 (1993).
3. S. Kleft and B. Kemper, *EMBO J.* **7**, 1527 (1988).
4. T. A. Kunkel, *Nature* **365**, 207 (1993).
5. L. S. Ripley, *Proc. Natl. Acad. Sci. U.S.A.* **79**, 4128 (1982).
6. T. A. H. Hjaalt and E. G. H. Wagner, *Nucleic Acids Res.* **23**, 580 (1995).
7. I. H. Goldberg and L. S. Kappen, in *Enediyne Antibiotics as Antitumor Agents*, D. B. Borders and T. W. Doyle, Eds. (Dekker, New York, 1994), pp. 327–362, and references therein; C. Nicolaou *et al.*, *Science* **256**, 1172 (1992).
8. L. S. Kappen and I. H. Goldberg, *Science* **261**, 1319 (1993); *Biochemistry* **32**, 13138 (1993).
9. ———, *Biochemistry* **34**, 5997 (1995).
10. A. Stassinopoulos and I. H. Goldberg, *ibid.*, p. 15359.
11. O. D. Hensens *et al.*, *Proc. Natl. Acad. Sci. U.S.A.* **91**, 4534 (1994); O. D. Hensens *et al.*, *J. Am. Chem. Soc.* **115**, 11030 (1993).
12. C. F. Yang, A. Stassinopoulos, I. H. Goldberg, *Biochemistry* **34**, 2267 (1995).
13. NCSi-gb was prepared on a milligram scale from **1** by an improvement of the previously reported method (*11*). The synthesis of the oligonucleotide was as reported previously (*12*).
14. M. Durand *et al.*, *Nucleic Acids Res.* **18**, 6353 (1990).
15. X. Gao, A. Stassinopoulos, J. S. Rice, I. H. Goldberg, *Biochemistry* **34**, 40 (1995).
16. K. Wüthrich, *NMR of Proteins and Nucleic Acids* (Wiley, New York, 1986).
17. In NOESY ($D_2O$) aromatic base–H1′, H2′/H2″ sequential NOEs are interrupted at the A5-T6 (residues across from the bulge site) and T13-T14 steps and are extremely weak at the A11-A12 and A12-T13 steps.
18. G. J. Quigley *et al.*, *Proc. Natl. Acad. Sci. U.S.A.* **77**, 7204 (1980); X. Gao and D. J. Patel, *Q. Rev. Biophys.* **22**, 93 (1989); M. Hansen, S. Yun, L. Hurley, *Chem. Biol.* **2**, 229 (1995).
19. G. M. Crippen, *Distance Geometry and Conformational Calculations* (Wiley, New York, 1981); J. Kuszewski, M. Nilges, A. T. Brünger, *J. Biomol. NMR* **2**, 33 (1992).
20. A. T. Brünger, G. M Clore, A. M. Gronenborn, M. Karplus, *Proc. Natl. Acad. Sci. U.S.A.* **83**, 3801 (1986); M. Nilges, G. M. Clore, A. M. Gronenborn, *FEBS Lett.* **239**, 129 (1988).
21. We used NOESY spectra (70-, 140-, and 250-ms mixing times) to derive distances using two-spin approximation or volume restraints. COSY-35 and double quantum filtered (DQF)–COSY data were used to derive δ (C5′-C4′-C3′-O3′) dihedral angle restraints (*16*). The iterative protocols used in the distance geometry and restrained molecular dynamics calculations were similar to those described previously (*15, 20*). Calculation statistics are as follows: root mean square deviation (RMSD) (590 NOE distance restraints), 0.3405 Å; $r^{1/6}$ (overall volume restraints), $9.841 \times 10^{-2}$; RMSD (39 dihedral angle restraints), 1.7445°; RMSD (six structure Cartesian coordinate files), 0.4862 Å; RMSD (chemical bonds), $4.197 \times 10^{-4}$ Å; RMSD (bond angles), 1.839°.
22. M. Nilges, J. Habazettl, A. T. Brünger, T. A. Holak, *J. Mol. Biol.* **219**, 499 (1991); T. James, *Curr. Opin. Struct. Biol.* **4**, 275 (1994).
23. Free DNA shows very weak sequential NOEs for the A12 and T13 bulged residues, as well as broadening of the resonances for their protons. These observations are consistent with a fluxional A12 and T13 bulged region with aromatic bases rotating in and out of the helix, distinctly different from a stable intrahelical A2 bulge, which has been shown to give well-defined NOE cross peaks [M. A. Rosen, D. Live, D. J. Patel, *Biochemistry* **31**, 4004 (1992)].
24. The structure of the DNA in the complex is heterogeneous. Its positive inclination and displacement from the helical axis are closer to A- than B-DNA values. Although the δ angles are mostly B-like, the sugar pucker reflected by the phase angles is consistent with a range of sugar conformations [W. Saenger, *Principles of Nucleic Acid Structure* (Springer-Verlag, New York, 1984)].
25. S. A. Woodson and D. M. Crothers, *Biochemistry* **27**, 3130 (1988); A. Bhattacharyya and D. M. J. Lilley, *Nucleic Acids Res.* **17**, 6821 (1989); J. A. Rice and D. M. Crothers, *Biochemistry* **28**, 4512 (1989).
26. For other efforts to find structure-specific nucleic acid interactive drugs see the following: W. D.Wilson *et al.*, *New J. Chem.* **18**, 419 (1994); and A. Slama-Schwok *et al.*, *J. Am. Chem. Soc.* **117**, 6822 (1995). Our structure contrasts with the one expected with simple intercalators that bind nonspecifically and nonexclusively at sites of single-base bulges [J. W. Nelson and I. Tinoco Jr., *Biochemistry* **24**, 6416 (1985); S. A. White and D. E. Draper, *Nucleic Acids Res.* **15**, 4049 (1987); L. D. Williams and I. H. Goldberg, *Biochemistry* **27**, 3004 (1988)]. Similarly, polyaromatic chemical carcinogens covalently adducted to a DNA base can intercalate at duplex and bulge sites [L. M. Eckel and T. R. Krugh, *Biochemisty* **33**, 13611 (1994); B. Mao *et al.*, *ibid.* **34**, 6226 (1995); B. Mao *et al.*, *ibid.*, p. 16641]. A solution structure of the complex formed between the intercalating antibiotic nogalamycin and a single-base bulge near the end of an oligonucleotide has recently been reported in which the drug acts as a duplex rather than a bulge binder because it obliterates the bulge by forcing base slippage [J. Caceres-Cortes and A. H.-J. Wang, *Biochemistry* **35**, 616 (1996)].
27. A conformation change that brings the C2 and C8″ closer, induced by movement of the DNA in the complex, can be neither excluded nor proven with our data (*8, 11*). No significant amounts of **4** are produced in the absence of bulged DNA substrate.


28. This work was supported by U.S. Public Health Service grants CA 44257 and GM 53793 and from NIH to I.H.G., and an American Cancer Society grant JFRA-493 to X.G. The use of the Keck NMR and Computation Center at the University of Houston is acknowledged.

29 February 1996; accepted 14 May 1996